

Production rates of dark photons and Z' in the Sun and stellar cooling bounds

Shao-Ping Li^a and Xun-Jie Xu^a

^a*Institute of High Energy Physics, Chinese Academy of Sciences, Beijing 100049, China*

E-mail: spli@ihep.ac.cn, xuxj@ihep.ac.cn

ABSTRACT: Light weakly interacting particles could be copiously produced in the Sun which, as a well-understood star, could provide severe constraints on such new physics. In this work, we calculate the solar production rates of light gauge bosons (e.g. dark photon) arising from various $U(1)$ extensions of the standard model. It is known that the dark photon production rate is suppressed by the dark photon mass if it is well below the plasmon mass of the medium. We show that for more general $U(1)$ gauge bosons, this suppression is absent if the couplings are not in alignment with those of the photon. We investigate a few frequently discussed $U(1)$ models including $B - L$, $L_\mu - L_\tau$, and $L_e - L_{\mu(\tau)}$, and derive the stellar cooling bounds for these models.

Contents

1	Introduction	1
2	Generic dark gauge boson	2
2.1	Interactions in the original and physical bases	2
2.2	The dark photon model: the photon-like and the hypercharge limits	4
2.3	The simplified dark photon model: the decoupling limit	5
3	Production of Z' in the Sun	6
3.1	The vanishing production rate of a photon-like Z'	6
3.2	The production rate of a generic Z'	8
3.3	Including the neutron- Z' coupling	10
4	Stellar cooling bounds for various $U(1)_X$ models	11
5	Conclusions	14
A	Transformation from the original basis to the physical basis	15
B	Medium-induced kinetic mixing rederived from coherent scattering	16

1 Introduction

New physics beyond the Standard Model (SM) may be hidden at low-energy scales with weak couplings to the SM. Dark photons or, more generally, dark neutral gauge bosons arising from $U(1)$ extensions of the SM are extensively studied cases of such new physics, with rising interest recently at the intensity frontier¹ and in cosmology [15–21]. Notably, they are also considered as popular dark matter candidates with interesting low-energy observational consequences [22, 23].

Hot and dense astrophysical environments can be used to probe light and weakly-coupled particles if they are copiously produced via frequent collisions of medium particles. In well-modeled stars such as the Sun, the additional energy loss caused by the emission of such new particles has been used to impose one of the most restrictive bounds on them in certain mass ranges [24–41]. In supernovae and neutron stars, new particles of higher masses could be probed [26–28, 42–50], though the astrophysical models have more diverse and larger uncertainties.

¹See [1–6] for reviews. In particular, searching for dark photons has been one of the major scientific goals of many ongoing or upcoming experiments like Belle-II [7], FASER [8, 9], SHiP [10], SeaQuest [11, 12], MATHUSLA [13, 14], etc.

It is known that the production rate of a very light dark photon in a thermal medium is suppressed by its mass [29–31]. In fact, in the massless limit due to mass degeneracy with the SM photon, one can always find a basis in which the dark photon is fully decoupled from the SM. Hence, the low-mass suppression is expected.

In this work, we would like to point out that the low-mass suppression is a generic feature for any gauge bosons with photon-like couplings, i.e., couplings to medium particles being proportional to their electric charges. However, if the couplings are not photon-like, which is also common in many $U(1)$ extensions of the SM (e.g. $B - L$ [51–53], $L_e - L_\mu$ [54–56]), then the low-mass suppression is absent. In this case, the production rate becomes independent of the mass in the low-mass limit. It is worth mentioning that even for the dark photon model the couplings should slightly deviate from the aforementioned photon-like scenario², though the effect of this deviation turns out to be negligible.

In addition to the dark photon model, we investigate a few popular $U(1)$ extensions including $B - L$, $L_\mu - L_\tau$, $L_e - L_\mu$, and $L_e - L_\tau$ which have been frequently considered in the literature in recent years [57–71]. Among these $U(1)$ models, the low-mass suppression is present for $L_\mu - L_\tau$ but not for $B - L$ and $L_e - L_{\mu(\tau)}$. Consequently, the stellar cooling bounds for these models have their respective very different low-mass limits.

This paper is organized as follows. In Sec. 2, we formulate the most general $U(1)$ extension of the SM, derive interactions of the new gauge boson (generically denoted by Z') in the physical basis, and discuss when the Z' features photon-like couplings. In Sec. 3, we calculate the production rate of Z' in the solar medium, with the focus on when and how the rate would vanish in the massless limit. Then in Sec. 4, we apply the calculations to a few $U(1)$ models and derive the corresponding stellar coupling bounds. Finally we conclude in Sec. 5 and relegate some details to the appendix.

2 Generic dark gauge boson

In our framework, we consider a generic dark gauge boson arising from a generic $U(1)$ extension of the SM, $SU(3)_c \times SU(2)_L \times U(1)_Y \times U(1)_X$. Such a gauge boson is called the dark photon if it couples to the SM content only via the kinetic mixing with the photon [72]. It is also generically referred to as Z' , defined rather broadly as a new neutral gauge boson similar to the SM Z boson. Although for historical reasons Z' is often considered to be around or above the electroweak scale [73], it can be light as well. We regard the dark photon as a special case of Z' and throughout this paper, use Z' as a more generic name and notation inclusively.

2.1 Interactions in the original and physical bases

In the original basis, the Lagrangian of relevant kinetic terms reads:

$$\mathcal{L} \supset -\frac{1}{4}W_{\mu\nu}W^{\mu\nu} - \frac{1}{4}\hat{B}_{\mu\nu}\hat{B}^{\mu\nu} - \frac{1}{4}\hat{X}_{\mu\nu}\hat{X}^{\mu\nu} - \frac{\epsilon}{2}\hat{B}_{\mu\nu}\hat{X}^{\mu\nu} + \sum_{\psi} \bar{\psi}\gamma^\mu iD_\mu\psi, \quad (2.1)$$

²When considering the SM gauge invariance which only allows for kinetic mixing with the SM $U(1)_Y$ gauge field, the dark photon should also slightly mix with the Z boson, which causes the small deviation—see Sec. 2.2 for a detailed discussion.

where W , B , and X denote the gauge field strength tensors of $SU(2)_L$, $U(1)_Y$, and $U(1)_X$, respectively. We add hats “ $\hat{}$ ” on two of them to remind the reader that their kinetic terms are not canonical in the original basis. The last term of Eq. (2.1) in which ψ is a SM fermion gives rise to the interactions of gauge bosons with fermions. The covariant derivative is defined as

$$D_\mu \equiv \partial_\mu - ig \sum_{a=1}^3 \frac{\sigma_a}{2} W_{a,\mu} - ig' Q_Y \hat{B}_\mu - ig_{Z'} Q_X \hat{X}_\mu, \quad (2.2)$$

where Q_Y and Q_X denote the charges of ψ under $U(1)_Y$ and $U(1)_X$.

Since the kinetic terms are not canonical due to the $\epsilon \hat{B}_{\mu\nu} \hat{X}^{\mu\nu}$ term, one needs to perform a linear (non-unitary) transformation to canonicalize the kinetic terms, for the applicability of the standard Feynman rules. We denote the fields after such a transformation by notations without hats ($\hat{X} \rightarrow X$, $\hat{B} \rightarrow B$). On the other hand, similar to the well-known fact of the SM that W_3 and B are not in the mass eigenbasis, here mass mixing among W , B , and X after symmetry breaking is generally expected. So a subsequent unitary (orthogonal) transformation is needed to obtain the physical states of gauge bosons with well-defined masses. Among them, there must be a massless state, which is defined as the photon, A .³ There should also be two massive neutral states. We denote them by Z and Z' , their masses by m_Z and $m_{Z'}$, and the ratio $r_m \equiv m_{Z'}^2/m_Z^2$.

We refer to the basis in which all gauge bosons are mass eigenstates with canonical kinetic terms as *the physical basis*. It is connected to the original basis via

$$(W_1, W_2, A, Z, Z')^T = \mathbb{T}(W_1, W_2, W_3, \hat{B}, \hat{X})^T, \quad (2.3)$$

where \mathbb{T} is a 5×5 matrix combining the aforementioned transformations. Its specific form is derived and presented in Appendix A.

Applying the transformation (2.3) to Eq. (2.2), one obtains the gauge interactions in the physical basis. According to Appendix A, the gauge interactions of A (photon) remain exactly the same as the SM ones, while for Z and Z' , the gauge interactions are given by

$$\mathcal{L} \supset g_Z^{(\psi)} \bar{\psi} \not{Z} \psi + g_{Z'}^{(\psi)} \bar{\psi} \not{Z}' \psi, \quad (2.4)$$

where $g_Z^{(\psi)}$ and $g_{Z'}^{(\psi)}$ are listed in Tab. 1, assuming the kinetic mixing term is the only source of the mass mixing. One should note that this assumption is valid only when Z' obtains its mass via the Stückelberg mechanism [74, 75] or the Higgs mechanism with SM singlet scalars that are only charged under $U(1)_X$. For the Higgs mechanism involving e.g. Higgs doublets charged under both $U(1)_X$ and $SU(2)_L \times U(1)_Y$, $g_Z^{(\psi)}$ and $g_{Z'}^{(\psi)}$ would involve an additional independent mass mixing parameter θ . We refer to Eqs. (A.11) and (A.12) in Appendix A for the results in this case.

³Since it is also conventional to denote the photon by γ , we use both γ and A interchangeably. The latter is more appropriate if Lorentz indices need to be explicit (e.g. A^μ) and the former is more commonly used in reaction processes (e.g. $e^- + p \rightarrow e^- + p + \gamma$).

ψ	$g_Z^{(\psi)}$	$g_{Z'}^{(\psi)}$
e_L	$\frac{g}{c_W} \left(s_W^2 - \frac{1}{2} \right) + \epsilon g_X^{(\psi)} \frac{s_W}{1-r_m}$	$g_X^{(\psi)} + \epsilon g s_W \frac{2c_W^2 - r_m}{2c_W(1-r_m)}$
e_R	$\frac{g}{c_W} \left(s_W^2 - \frac{1}{2} \right) + \epsilon g_X^{(\psi)} \frac{s_W}{1-r_m}$	$g_X^{(\psi)} + \epsilon g s_W \frac{c_W^2 - r_m}{c_W(1-r_m)}$
u_L	$\frac{2g}{3c_W} \left(\frac{3}{4} - s_W^2 \right) + \epsilon g_X^{(\psi)} \frac{s_W}{1-r_m}$	$g_X^{(\psi)} - \epsilon g s_W \frac{4c_W^2 - r_m}{6c_W(1-r_m)}$
u_R	$\frac{2g}{3c_W} \left(-s_W^2 \right) + \epsilon g_X^{(\psi)} \frac{s_W}{1-r_m}$	$g_X^{(\psi)} - \epsilon g s_W \frac{2(c_W^2 - r_m)}{3c_W(1-r_m)}$
d_L	$\frac{g}{3c_W} \left(s_W^2 - \frac{3}{2} \right) + \epsilon g_X^{(\psi)} \frac{s_W}{1-r_m}$	$g_X^{(\psi)} + \epsilon g s_W \frac{2c_W^2 + r_m}{6c_W(1-r_m)}$
d_R	$\frac{g}{3c_W} s_W^2 + \epsilon g_X^{(\psi)} \frac{s_W}{1-r_m}$	$g_X^{(\psi)} + \epsilon g s_W \frac{c_W^2 - r_m}{3c_W(1-r_m)}$
ν_L	$\frac{g}{2c_W} + \epsilon g_X^{(\psi)} \frac{s_W}{1-r_m}$	$g_X^{(\psi)} - \epsilon g s_W \frac{r_m}{2c_W(1-r_m)}$
ν_R	$\epsilon g_X^{(\psi)} \frac{s_W}{1-r_m}$	$g_X^{(\psi)}$

Table 1. Effective couplings of Z and Z' in the $SU(2)_L \times U(1)_Y \times U(1)_X$ model assuming that the kinetic mixing term is the only source of mass mixing. Here $r_m \equiv m_{Z'}/m_Z^2$, $g_X^{(\psi)} \equiv g_{Z'} Q_X^{(\psi)}$ with $g_{Z'}$ and $Q_X^{(\psi)}$ defined in Eq. (2.2). Since some models such as $U(1)_{B-L}$ may introduce right-handed neutrinos (ν_R), we also include ν_R here for completeness.

2.2 The dark photon model: the photon-like and the hypercharge limits

In our work, the dark photon model is defined as a special case of the above model: either $Q_X^{(\psi)} = 0$ or $g_{Z'}$ is negligibly small. Hence the gauge interactions in the physical basis can be obtained by taking $g_X^{(\psi)} \equiv g_{Z'} Q_X^{(\psi)} \rightarrow 0$ in Tab. 1. Here we would like to outline two interesting limits in the dark photon model.

- The photon-like limit. For a very light Z' , we take the limit $r_m \rightarrow 0$ in Tab. 1 with $g_X^{(\psi)} = 0$ and obtain

$$g_{Z'}^{(\psi)} = -\epsilon e c_W Q_{\text{em}}^{(\psi)}, \quad \text{i.e. } g_{Z'}^{(\psi)} \propto Q_{\text{em}}^{(\psi)}, \quad (2.5)$$

where $e = g s_W$ and $Q_{\text{em}}^{(\psi)}$ is the electric charge of ψ . Eq. (2.5) implies that in the zero mass limit, the interactions of Z' with fermions are very similar to the interactions of the photon in the sense that $(g_{Z'}^{(e)} : g_{Z'}^{(\nu)} : g_{Z'}^{(u)} : g_{Z'}^{(d)}) = (-1 : 0 : 2/3 : -1/3)$.

- The hypercharge limit. For a heavy Z' with the mass well above the electroweak scale, we take the limit $r_m \rightarrow \infty$ together with $g_X^{(\psi)} = 0$ in Tab. 1 and obtain

$$g_{Z'}^{(\psi)} = \epsilon g \frac{s_W}{c_W} Q_Y^{(\psi)}, \quad \text{i.e. } g_{Z'}^{(\psi)} \propto Q_Y^{(\psi)}. \quad (2.6)$$

For example, in this limit we have $(g_{Z'}^{(e_L, \nu_L)} : g_{Z'}^{(e_R)} : g_{Z'}^{(u_L, d_L)}) = (-1/2 : -1 : 1/6)$. This is expected because at high energies the electroweak symmetry is restored and Z' essentially mixes only with the SM $U(1)_Y$ gauge field.

2.3 The simplified dark photon model: the decoupling limit

In the literature, it is quite common that only the kinetic mixing between \hat{X} and the photon (\hat{A}) is considered:

$$\mathcal{L} \supset -\frac{1}{4}\hat{A}_{\mu\nu}\hat{A}^{\mu\nu} - \frac{1}{4}\hat{X}_{\mu\nu}\hat{X}^{\mu\nu} - \frac{\varepsilon}{2}\hat{A}_{\mu\nu}\hat{X}^{\mu\nu} + eJ_{\text{em}}^\mu\hat{A}_\mu + \frac{1}{2}m_X^2\hat{X}_\mu\hat{X}^\mu, \quad (2.7)$$

where $\varepsilon \equiv \epsilon c_W$ and J_{em}^μ is the electromagnetic current. This Lagrangian is not gauge invariant and we refer to it as *the simplified dark photon model*. Disregarding the gauge invariance issue, it can concisely capture the main feature of the complete model in the low- $m_{Z'}$ limit, i.e. the photon-like limit in Sec. 2.2.

In the simplified dark photon model, the transformation in Eq. (2.3) is reduced to $(A, Z')^T = \mathbb{T}(\hat{A}, \hat{X})^T$ with

$$\mathbb{T} = \begin{pmatrix} 1 & \varepsilon \\ 0 & \sqrt{1-\varepsilon^2} \end{pmatrix}. \quad (2.8)$$

And the kinetic, mass, and gauge interaction terms are transformed as follows:

$$\text{kinetic matrix : } K = \begin{pmatrix} 1 & \varepsilon \\ \varepsilon & 1 \end{pmatrix} \xrightarrow{\mathbb{T}} \begin{pmatrix} 1 & 0 \\ 0 & 1 \end{pmatrix}, \quad (2.9)$$

$$\text{mass matrix : } M^2 = \begin{pmatrix} 0 & 0 \\ 0 & m_X^2 \end{pmatrix} \xrightarrow{\mathbb{T}} \begin{pmatrix} 0 & 0 \\ 0 & m_{Z'}^2 \end{pmatrix}, \quad m_{Z'}^2 = \frac{m_X^2}{1-\varepsilon^2}, \quad (2.10)$$

$$\text{current matrix : } J = \begin{pmatrix} J_{\text{em}} \\ 0 \end{pmatrix} \xrightarrow{\mathbb{T}} J_{\text{em}} \begin{pmatrix} 1 \\ x \end{pmatrix}, \quad x = \frac{-\varepsilon}{\sqrt{1-\varepsilon^2}}, \quad (2.11)$$

where matrices K , M^2 and J are defined by rewriting Eq. (2.7) as $\mathcal{L} \supset -\frac{1}{4}V_{\mu\nu}^TKV^{\mu\nu} + J_\mu^TV^\mu + \frac{1}{2}V_\mu^TM^2V^\mu$ with $V_\mu = (\hat{A}_\mu, \hat{X}_\mu)^T$.

It is important to notice that \mathbb{T} is unique if one requires that it simultaneously diagonalizes K and M^2 . However, if $m_X^2 = 0$, then \mathbb{T} is no longer unique, because if $\mathbb{T} \rightarrow \mathbb{T}' = \mathbb{O} \cdot \mathbb{T}$ with \mathbb{O} an arbitrary orthogonal matrix ($\mathbb{O} \cdot \mathbb{O}^T = 1$), Eq. (2.9) remains the same while $M^2 = 0$ is unchanged. In other words, the physical basis in which all gauge bosons are mass eigenstates is no longer unique due to the mass degeneracy. In this particular case, one could further choose an appropriate \mathbb{O} so that

$$K = \mathbb{T}'^T \begin{pmatrix} 1 & 0 \\ 0 & 1 \end{pmatrix} \mathbb{T}', \quad M^2 = 0, \quad J \propto \mathbb{T}'^T \begin{pmatrix} 1 \\ 0 \end{pmatrix}, \quad (2.12)$$

which implies that under this basis, the dark degree of freedom is fully decoupled from the SM. We refer to this as the decoupling limit. Since physical results should be basis independent, when computing e.g. stellar energy loss rates in other bases where Z' is superficially coupled to J_{em} , some cancellations in the final results are expected, as will be shown explicitly in our calculation in Sec. 3.1.

A further generalization, which to our knowledge has not been noticed in the literature, is that even if the lower component of J in Eq. (2.11) is nonzero, one can still rotate it away in the zero mass limit so that a massless Z' is fully decoupled. This is possible if

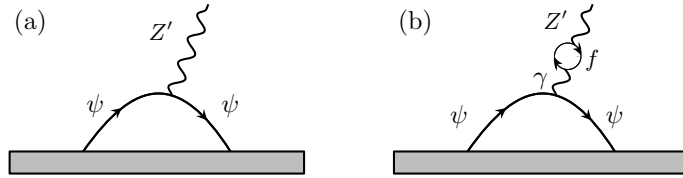


Figure 1. A generic diagram for Z' production (left) accompanied with another diagram (right) which is equally important in a thermal or dense medium. The gray boxes represent remaining parts of the diagrams, which can be quite arbitrary.

\hat{X} is originally coupled to SM fermions ($Q_X^{(\psi)} \neq 0$) but the corresponding current, J_X , is proportional to J_{em} (i.e. $J_X^\mu \propto 2/3\bar{u}\gamma^\mu u - 1/3\bar{d}\gamma^\mu d - \bar{e}\gamma^\mu e + \dots$). This will also be shown in the next section.

3 Production of Z' in the Sun

3.1 The vanishing production rate of a photon-like Z'

It is known that the dark photon production rate in a finite-temperature environment vanishes in the limit of zero mass [29–31, 33]. This feature can be understood from the decoupling limit discussed in Sec. 2.3.

Here we would like to make a generalization that this is also true for other Z' with photon-like couplings. For instance, in plasma consisting of only protons and electrons, the Z' in the $U(1)_{B-L}$ model has $g_{Z'}^{(p)} = -g_{Z'}^{(e)}$, which makes the relevant couplings photon-like. Consequently, its production rate vanishes in the $m_{Z'} \rightarrow 0$ limit [33].

Below we show explicitly how it vanishes for a photon-like Z' . In previous studies, this feature is shown for the dark photon in the basis of $\hat{\mathbf{V}}$ where the gauge bosons are not in mass eigenstates. Here we adopt the physical basis (\mathbf{V}_{ph}) for a rigorous treatment.

Consider a generic Feynman diagram for Z' production, as shown in the left panel of Fig. 1. Since in the physical basis there is no mixing between any gauge bosons, the final-state Z' has to be attached to a fermion ψ in the diagram. Hence the diagram should be proportional to the coupling $g_{Z'}^{(\psi)}$.

On the other hand, such a diagram is always accompanied with another diagram shown in the right panel of Fig. 1. This diagram would be just a higher-order correction in vacuum, but in a thermal or dense medium it can be equally important. It is known that coherent scattering of photons with charged particles in a medium modifies the photon dispersion relation. In plasma, this corresponds to the well-known plasmon masses. In a transparent medium, this gives rise to the refractive index. The medium effect can be calculated by evaluating the self-energy loop of the photon using finite-temperature/density field theories. Alternatively, one can compute the medium effect using the coherent scattering theory—see Appendix B for a re-derivation. If the final-state photon is changed to Z' , one obtains medium-induced mixing between Z' and the photon [76]. *Therefore, even though we have removed all mixing between gauge bosons in vacuum, the medium effect still causes additional mixing.*

The medium-induced mixing between γ and Z' can be computed by rescaling the self-energy of the photon in the medium:

$$\Pi_{\gamma-(f)-Z'}^{\mu\nu} = \frac{g_{Z'}^{(f)}}{eQ_{\text{em}}^{(f)}} \Pi_{\gamma-(f)-\gamma}^{\mu\nu}, \quad (3.1)$$

where $\Pi_{\gamma-(f)-\gamma}^{\mu\nu}$ denotes the photon self-energy, with f the charged fermion running in the loop. The self-energy $\Pi_{\gamma-(f)-\gamma}^{\mu\nu}$ is conventionally decomposed as

$$\Pi_{\gamma-(f)-\gamma}^{\mu\nu} = \Pi_{\gamma-(f)-\gamma}^L \epsilon_L^\mu \epsilon_L^{*\nu} + \Pi_{\gamma-(f)-\gamma}^T (\epsilon_{T1}^\mu \epsilon_{T1}^{*\nu} + \epsilon_{T2}^\mu \epsilon_{T2}^{*\nu}), \quad (3.2)$$

where ϵ_L and $\epsilon_{T1,2}$ are the longitudinal and two transverse polarization vectors, and $\Pi_{\gamma-(f)-\gamma}^{L,T}$ in non-degenerate and non-relativistic plasma can be found in Refs. [26, 33, 77]⁴:

$$\Pi_{\gamma-(f)-\gamma}^T \approx Q_f^2 \frac{e^2 n_f}{m_f}, \quad \Pi_{\gamma-(f)-\gamma}^L \approx Q_f^2 \left(1 - \frac{|\mathbf{k}|^2}{\omega^2}\right) \frac{e^2 n_f}{m_f}. \quad (3.3)$$

Here the photon momentum is $k^\mu = (\omega, \mathbf{k})$; n_f , m_f , and Q_f are the number density, mass, and electric charge of f ,⁵ respectively.

Now applying the in-medium photon self-energy and γ - Z' mixing to the second diagram in Fig. 1, we obtain

$$\text{diagram (b)} \propto eQ_{\text{em}}^{(\psi)} \cdot \frac{-i}{k^2 - \Pi_{\gamma\gamma}^{L,T}} \cdot i\Pi_{\gamma Z'}^{L,T}, \quad (3.4)$$

where

$$\Pi_{\gamma\gamma}^{L,T} \equiv \sum_f \Pi_{\gamma-(f)-\gamma}^{L,T}, \quad \Pi_{\gamma Z'}^{L,T} \equiv \sum_f \Pi_{\gamma-(f)-Z'}^{L,T}. \quad (3.5)$$

For photon-like Z' couplings, $g_{Z'}^{(f)} \propto eQ_{\text{em}}^{(f)}$, let us define a universal ratio r_g between them,

$$g_{Z'}^{(f)} = r_g eQ_{\text{em}}^{(f)}, \quad (3.6)$$

so that $\Pi_{\gamma Z'}^{L,T} = r_g \Pi_{\gamma\gamma}^{L,T}$. Therefore, the two diagrams in Fig. 1 can be combined to give

$$\begin{aligned} \text{diagrams (a) + (b)} &\propto g_{Z'}^{(\psi)} + eQ_{\text{em}}^{(\psi)} \frac{r_g \Pi_{\gamma\gamma}^{L,T}}{k^2 - \Pi_{\gamma\gamma}^{L,T}} \\ &\propto g_{Z'}^{(\psi)} \left[1 + \frac{\Pi_{\gamma\gamma}^{L,T}}{m_{Z'}^2 - \Pi_{\gamma\gamma}^{L,T}} \right] \\ &\propto g_{Z'}^{(\psi)} \frac{m_{Z'}^2}{m_{Z'}^2 - \Pi_{\gamma\gamma}^{L,T}}, \end{aligned} \quad (3.7)$$

which implies that the two diagrams cancel out in the $m_{Z'}^2 \rightarrow 0$ limit, provided that $\Pi_{\gamma\gamma}^{L,T}$ is finite. This conclusion only relies on Eq. (3.6), irrespective of the specific forms of $\Pi_{\gamma\gamma}^{L,T}$.

⁴Note that at the one-loop level, $\Pi_{\gamma-(f)-\gamma}^{L,T}$ are real. Their imaginary parts, which are related to the thermal production rate of γ , only arise at two-loop or higher levels.

⁵Here the fermion f should be unbound particles (such as electrons and ions in the plasma). Charged particles in bound states such as quarks in protons or protons in helium should not be taken into account individually.

3.2 The production rate of a generic Z'

For a generic Z' with the couplings disproportional to the electric charges, the aforementioned cancellation is generally absent. For simplicity, let us first consider ionized hydrogen as the medium, which is composed of only free electrons and protons. We introduce the following κ parameter to quantify the deviation from the photon-like scenario:

$$g_{Z'}^{(p)} : g_{Z'}^{(e)} = \kappa - 1 : 1. \quad (3.8)$$

Taking $\kappa = 0$ or 1 would correspond to a photon-like or baryophobic Z' . Using Eq. (3.8) and repeating the calculations in Sec. 3.1, we find that the final result in Eq. (3.7) for $\psi = e$ is changed to

$$\text{diagrams (a) + (b)} \propto g_{Z'}^{(e)} \frac{m_{Z'}^2 - \kappa \Pi_{\gamma-(p)-\gamma}^{L,T}}{m_{Z'}^2 - \Pi_{\gamma\gamma}^{L,T}}, \quad (3.9)$$

which becomes insensitive to $m_{Z'}^2$ if $m_{Z'}^2$ is well below $\kappa \Pi_{\gamma-(p)-\gamma}^{L,T}$ and $\Pi_{\gamma\gamma}^{L,T}$. Substituting Eq. (3.3) into Eq. (3.9) and assuming $\kappa \Pi_{\gamma-(p)-\gamma}^{L,T} < \Pi_{\gamma\gamma}^{L,T}$, we obtain

$$\text{diagrams (a) + (b)} \propto g_{Z'}^{(e)} \kappa \frac{m_p^{-1}}{m_e^{-1} + m_p^{-1}} \quad \text{for } m_{Z'}^2 \ll \kappa \frac{e^2 n_p}{m_p}. \quad (3.10)$$

In a homogeneous medium with infinite extent, the evolution of the Z' species is governed by the following Boltzmann equation:

$$\frac{df_{Z'}(\mathbf{k})}{dt} = \Gamma_{Z'}^{\text{gain}}(\mathbf{k}) (1 + f_{Z'}(\mathbf{k})) - \Gamma_{Z'}^{\text{loss}}(\mathbf{k}) f_{Z'}(\mathbf{k}), \quad (3.11)$$

where $f_{Z'}$ is the momentum distribution function of Z' , and $\Gamma_{Z'}^{\text{gain/loss}}$ is the gain/loss rate of Z' , to be determined by evaluating collision terms for specific processes. The $1 + f_{Z'}$ factor attached to $\Gamma_{Z'}^{\text{gain}}$ comes from quantum statistics.

For the photon γ , we define a similar gain/loss rate $\Gamma_{\gamma}^{\text{gain/loss}}$ and $\Gamma_{\gamma} \equiv \Gamma_{\gamma}^{\text{loss}} - \Gamma_{\gamma}^{\text{gain}}$. In the photon Boltzmann equation [similar to Eq. (3.11)], we have $df_{\gamma}/dt = 0$ due to thermal equilibrium and hence

$$\Gamma_{\gamma}^{\text{gain}} = f_{\gamma} \Gamma_{\gamma}, \quad \Gamma_{\gamma}^{\text{loss}} = (1 + f_{\gamma}) \Gamma_{\gamma}. \quad (3.12)$$

Due to the weak couplings and low production rate, Z' should be far from reaching thermal equilibrium, i.e. $f_{Z'} \ll 1$. Hence one can neglect the last term in Eq. (3.11) and take $\Gamma_{Z'}^{\text{gain}} (1 + f_{Z'}) \approx \Gamma_{Z'}^{\text{gain}}$ as the production rate. Under this assumption, Eq. (3.11) implies

$$\frac{dn_{Z'}}{dt} = \int \Gamma_{Z'}^{\text{gain}} \frac{d^3 \mathbf{k}}{(2\pi)^3}, \quad (3.13)$$

where $n_{Z'}$ is the number density of Z' .

According to Eq. (3.9), $\Gamma_{Z'}^{\text{gain}}$ can be related to the gain rate of the photon $\Gamma_{\gamma}^{\text{gain}}$ as follows:

$$\Gamma_{Z'}^{\text{gain}} = \left| \frac{g_{Z'}^{(e)} m_{Z'}^2 - \kappa \Pi_{\gamma-(p)-\gamma}^{L,T}}{e Q_{\text{em}}^{(e)} m_{Z'}^2 - \Pi_{\gamma\gamma}^{L,T}} \right|^2 \Gamma_{\gamma}^{\text{gain}}. \quad (3.14)$$

The photon gain rate $\Gamma_\gamma^{\text{gain}}$ consists of two dominant contributions, one from bremsstrahlung ($e^- + p \rightarrow e^- + p + \gamma$) and the other from Thomson/Compton scattering ($\gamma + e^- \rightarrow \gamma + e^-$). Including the two contributions, the explicit form of $\Gamma_\gamma^{\text{gain}}$ in the longitudinal mode reads [31, 33]:⁶

$$\Gamma_\gamma^{\text{gain}} = f_\gamma \frac{64\pi^2 \alpha^3 n_e n_p}{3\sqrt{2\pi T} m_e^{3/2} \omega^3} F(\omega/T) + f_\gamma \frac{8\pi \alpha^2 n_e}{3m_e^2} \sqrt{1 - \frac{e^2 n_e}{m_e \omega^2}} \Theta(\omega^2 - e^2 n_e/m_e), \quad (3.15)$$

where $\alpha \equiv e^2/(4\pi) \approx 1/137$, $f_\gamma = 1/(e^{\omega/T} - 1)$, Θ is the Heaviside theta function, and $F(x) \approx K_0(x/2) \sinh(x/2)$ assuming that the screening effect is negligible. For the transverse mode, the same expression in Eq. (3.15) can be used at the leading order [31].

The first and second terms in Eq. (3.15) are proportional to α^3 and α^2 , corresponding to the contributions of bremsstrahlung and Thomson/Compton scattering, respectively. It is noteworthy that despite its higher order in α , the first term is generally greater than the second, because the initial states of $e^- + p \rightarrow e^- + p + \gamma$ and $\gamma + e^- \rightarrow \gamma + e^-$ contain a proton and a photon, respectively, while the number density of the former is much higher than the latter. Taking the solar central temperature $T \sim 10^7 K$ and density $\rho \sim 150 \text{g/cm}^3$ [79] for example, we obtain $n_p \approx \rho/m_p \approx 9 \times 10^{25}/\text{cm}^3$ and $n_\gamma = 2\zeta(3)T^3/\pi^2 \approx 2 \times 10^{22}/\text{cm}^3$, i.e., n_p is $\sim 10^3$ higher than n_γ . This is enough to compensate the difference between α^3 and α^2 .

When using Eq. (3.14) to compute $\Gamma_{Z'}^{\text{gain}}$, one may encounter resonance production occurring at $m_{Z'}^2 \sim \Pi_{\gamma\gamma}^{L,T}$. To the order of α , $\Pi_{\gamma\gamma}^{L,T}$ are real and given by Eq. (3.3). To the order of α^2 or higher, $\Pi_{\gamma\gamma}^{L,T}$ contain nonzero imaginary parts, which can be determined using Weldon's formula [80]:

$$\text{Im}\Pi_{\gamma\gamma}^{L,T} = -\omega\Gamma_\gamma, \quad (3.16)$$

where Γ_γ can be computed using $\Gamma_\gamma^{\text{gain}} = f_\gamma\Gamma_\gamma$ and Eq. (3.15). With Eq. (3.16), Eq. (3.14) can be rewritten as

$$\Gamma_{Z'}^{\text{gain}} = C \frac{1}{\Delta^2 + \Gamma_\gamma^2} \Gamma_\gamma, \quad (3.17)$$

where $\Delta \equiv (m_{Z'}^2 - \text{Re}\Pi_{\gamma\gamma}^{L,T})/\omega$ and $C(\omega)$ absorbs unimportant quantities. The resonance occurs at $\Delta = 0$ and $\Gamma_{Z'}^{\text{gain}} = C/\Gamma_\gamma$. Despite that the height of the resonance is proportional to $1/\Gamma_\gamma$, the overall contribution of the resonance to the integrated production rate $\int \Gamma_\gamma^{\text{gain}} d^3\mathbf{k}$ is insensitive to Γ_γ , as previously pointed out in Ref. [30]. This can be understood by noticing that at a wide range (e.g. $\Delta \in [-K, K]$ with $K \gg \Gamma_\gamma$), Eq. (3.17) behaves like the Dirac delta function⁷, which is why the integrated contribution is insensitive to the height of the resonance.

⁶Comparing to Eq. (4.5) in Ref. [31], we have added an f_γ factor because $\Gamma_\gamma^{\text{gain}} = f_\gamma\Gamma_\gamma$. Ref. [33] adopted the thermally-averaged Gaunt factor [78] to compute the bremsstrahlung contribution—see Eqs. (A.5) and (A.6) therein. We have checked that this is equivalent to Eq. (4.5) in Ref. [31] if the screening effect is negligible.

⁷Recall that the Dirac delta function can also be defined as $\delta(x) = \frac{1}{\pi} \lim_{\Gamma \rightarrow 0} \frac{\Gamma}{x^2 + \Gamma^2}$, which is similar to the form of Eq. (3.17).

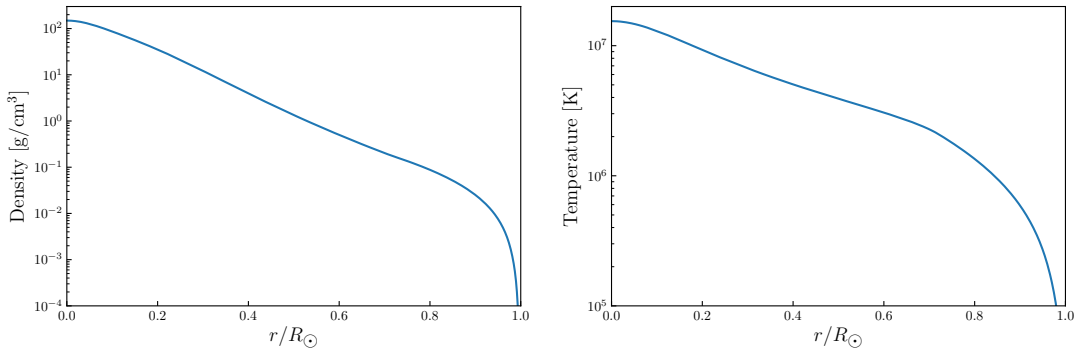


Figure 2. The solar density and temperature profiles used in this work. Data taken from Ref. [81].

In the Sun, Z' produced will immediately escape the finite extent of the medium. In this case, Eq. (3.13) should be interpreted as the number of Z' produced per unit volume per unit time in a local region. The temperature and the density of the medium decrease as the distance to the center r increases. Fig. 2 shows the variation of the temperature and the density with respect to r in the standard solar model. The data is taken from the latest calculation in Ref. [81] based on the AGSS09 solar model [82].

The total number of Z' produced in the Sun per unit time, dN/dt , and the total energy loss per unit time, dE_{loss}/dt , can be obtained by integrating Eq. (3.13) over the entire solar profile:

$$\frac{dN}{dt} = \int_0^{R_\odot} dr 4\pi r^2 \int_0^\infty dk \frac{k^2}{2\pi^2} \Gamma_{Z'}^{\text{gain}}, \quad (3.18)$$

$$\frac{dE_{\text{loss}}}{dt} = \int_0^{R_\odot} dr 4\pi r^2 \int_0^\infty dk \frac{\omega k^2}{2\pi^2} \Gamma_{Z'}^{\text{gain}}. \quad (3.19)$$

In Fig. 3, we show the energy loss rate dE_{loss}/dt computed using Eq. (3.19) for a few selected values of κ and $g_{Z'}^{(e)} = 10^{-15}$. Eq. (3.19) can be used to compute the contribution of each polarization mode. In Fig. 3 we sum over one longitudinal and two transverse modes. The results are normalized by the solar luminosity

$$L_\odot = 3.83 \times 10^{26} \text{ Watt}. \quad (3.20)$$

As is expected from Eq. (3.7), the energy loss rate vanishes in the photon-like limit ($\kappa = 0$, $m_{Z'} \rightarrow 0$) but if $\kappa \neq 0$, the curves in Fig. 3 become flat below certain mass scales, implying nonvanishing rates in the low-mass limit.

3.3 Including the neutron- Z' coupling

There is a considerably high abundance of neutrons in the Sun, mostly in the form of ^4He , ^{16}O , ^{14}C , and other heavy nuclei. Overall, the ratio of the number densities of neutrons and protons is $n_n/n_p \approx 17\%$. Hence if Z' is coupled to the neutron, its contribution is not negligible. To include this contribution, we modify Eq. (3.8) as follows

$$g_{Z'}^{(n)} : g_{Z'}^{(p)} : g_{Z'}^{(e)} = \kappa_n : \kappa - 1 : 1, \quad (3.21)$$

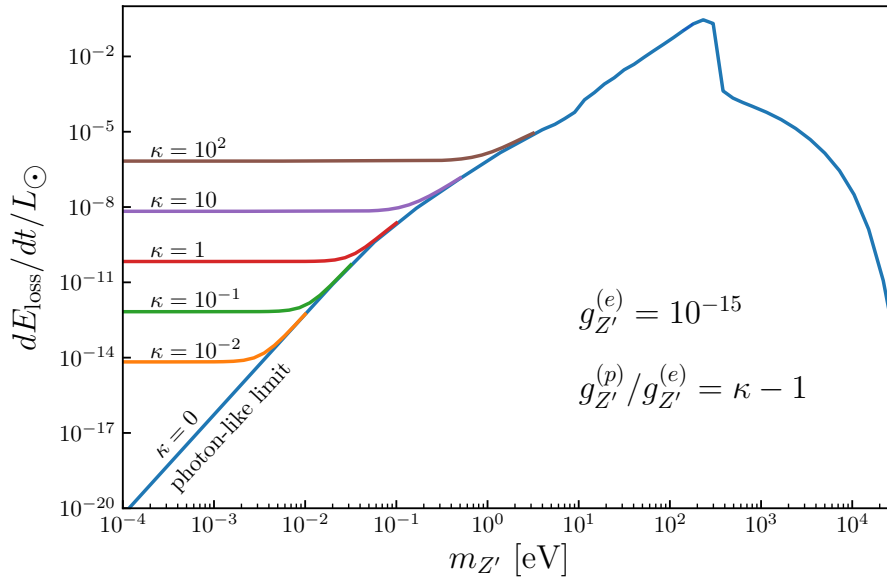


Figure 3. The energy loss rate caused by Z' emission in the Sun for different values of κ , which is defined by $g_{Z'}^{(p)}/g_{Z'}^{(e)} = \kappa - 1$. The rate vanishes in the photon-like limit ($\kappa = 0$, $m_{Z'} \rightarrow 0$) while increasing κ leads to a nonvanishing rate in the low-mass limit.

which introduces a new ratio κ_n .

Note that neutrons in the solar plasma are bound in nuclei and should not be treated as free particles (the same for $\sim 17\%$ of protons). For simplicity, we assume all neutrons are bound in ${}^4\text{He}$ and neglect elements heavier than ${}^4\text{He}$. Under this assumption, the plasma is composed of e^- , p , and ionized ${}^4\text{He}$. Then Eq. (3.9) is changed to

$$\text{diagrams (a) + (b)} \propto g_{Z'}^{(e)} \frac{m_{Z'}^2 - \kappa \Pi_{\gamma-(p)-\gamma}^{L,T} - (\kappa + \kappa_n) \Pi_{\gamma-({}^4\text{He})-\gamma}^{L,T}}{m_{Z'}^2 - \Pi_{\gamma\gamma}^{L,T}}, \quad (3.22)$$

where $\Pi_{\gamma-({}^4\text{He})-\gamma}^{L,T}$ takes the form in Eq. (3.3) with $n_f = n_n/2$ and $m_f = 2m_n + 2m_p \approx 4m_p$.

In particular, for the $B-L$ model ($\kappa_n = -1$, $\kappa = 0$), Eq. (3.22) reduces to

$$\text{diagrams (a) + (b)} \propto g_{Z'}^{(e)} \frac{m_{Z'}^2 + \Pi_{\gamma-({}^4\text{He})-\gamma}^{L,T}}{m_{Z'}^2 - \Pi_{\gamma\gamma}^{L,T}}, \quad (3.23)$$

which implies that the production rate is nonvanishing at $m_{Z'} \rightarrow 0$ due to the presence of ${}^4\text{He}$ in the Sun. This feature has been previously shown in Ref. [33]—see Fig. 4 therein.

To compute the production rate of a generic Z' , we only need to take Eq. (3.14) with the numerator $m_{Z'}^2 - \kappa \Pi_{\gamma-(p)-\gamma}^{L,T}$ replaced by the one in Eq. (3.22), and modify Eq. (3.15) with $n_e n_p \rightarrow n_e \sum_f Q_f^2 n_f$ where f in the sum runs over all relevant nucleus species.

4 Stellar cooling bounds for various $U(1)_X$ models

The standard solar model has been well established with a variety of predictions (e.g. solar neutrino fluxes) in good agreement with observations [79, 83]. In the presence of additional

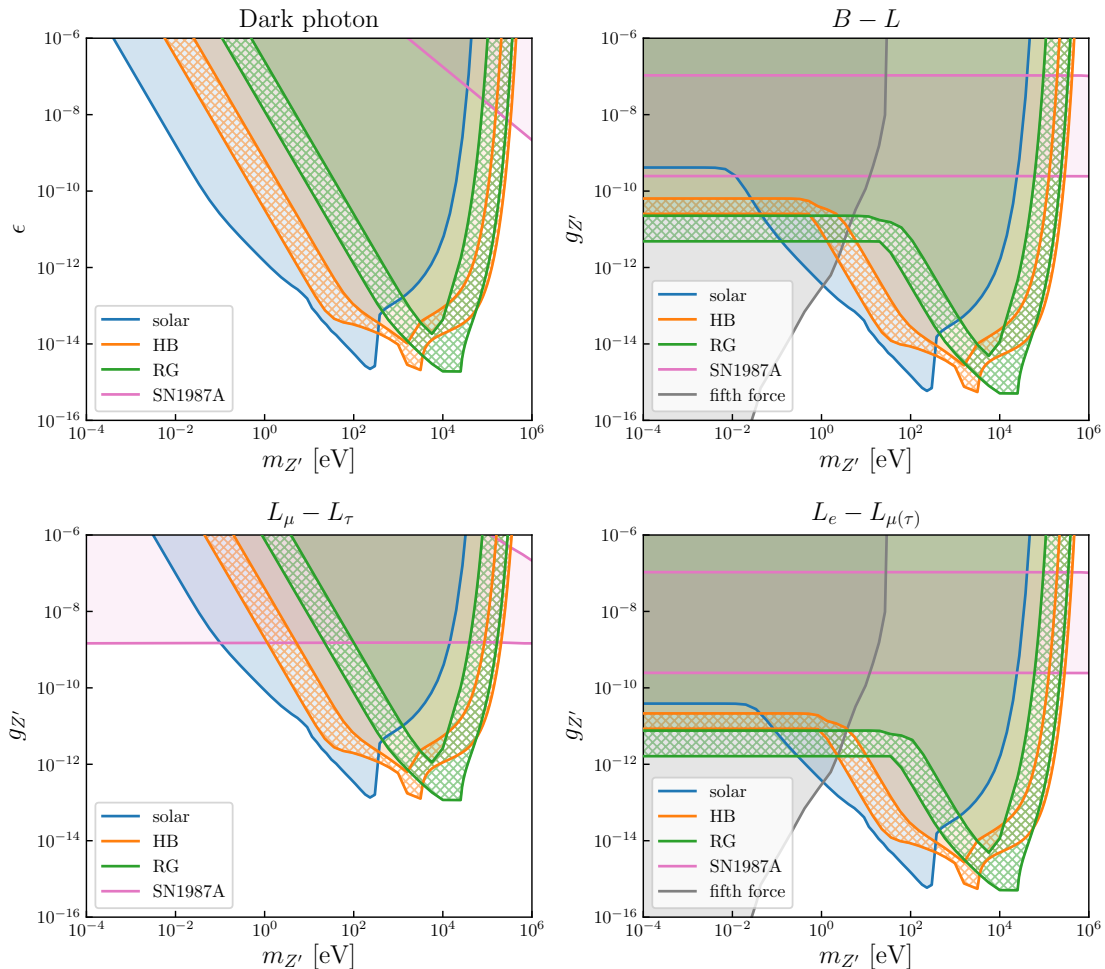


Figure 4. Stellar (Solar, HB, RG) cooling bounds on four $U(1)_X$ models compared with existing bounds (SN1987A and fifth force). For the $L_\mu - L_\tau$ model, we have used loop-induced couplings to electrons and protons—see Eq. (4.1). Curves in the right panels become flat below certain mass scales because $g_{Z'}^{(p)}/g_{Z'}^{(e)} \neq -1$ and/or $g_{Z'}^{(n)}/g_{Z'}^{(e)} \neq 0$, as discussed in the text. The supernova bounds (SN1987A) are taken from Refs. [45, 85]. The fifth-force bounds consist of laboratory limits from the inverse-square-law test of gravity and the Casimir effect, taken from Ref. [59]. They are absent in the left panels for photon-like couplings.

energy loss due to the emission of dark particles, many of its predictions could be altered. Without running dedicated simulations for the altered solar models, it is generally believed that one can take $dE_{\text{loss}}/dt \lesssim 10\%L_\odot$ as a conservative bound on the energy loss rate [31, 33, 84]. In our work, we also take $10\%L_\odot$ as the maximally allowed value of dE_{loss}/dt in the Sun.

We consider a few popular $U(1)_X$ models including the dark photon ($Q_X = 0$), the $B - L$ model which is the simplest flavor-universal anomaly-free $U(1)$ extension of the SM, and leptonic $U(1)$ extensions $L_\alpha - L_\beta$ with $\alpha, \beta \in \{e, \mu, \tau\}$. The $L_\mu - L_\tau$ model has gained rising interest due to its viability to accommodate the muon $g - 2$ anomaly after

combining all known bounds. Although Z' in this model does not couple to electrons and quarks directly, there are loop-induced couplings to all charged fermions [86]:

$$g_{Z'}^{(f)} = -\frac{\alpha}{3\pi} g_{Z'} Q_{\text{em}}^{(f)} \log\left(\frac{m_\mu^2}{m_\tau^2}\right). \quad (4.1)$$

Note that the loop-induced couplings are proportional to $Q_{\text{em}}^{(f)}$, which implies that these couplings are photon-like and hence the production rate vanishes at $m_{Z'} \rightarrow 0$. Eq. (4.1) is generated by loop diagrams with an internal photon mediator and a μ/τ fermion loop. If the photon mediator is replaced by the SM Z boson, one would get more suppressed loop-induced couplings. They are suppressed by $m_{Z'}^2/m_Z^2$ and hence negligible in our analysis.

For these models, we take the following values for κ and κ_n :

$$\text{dark photon : } (\kappa, \kappa_n) = (0, 0), \quad g_{Z'}^{(e)} = ec_W \epsilon, \quad (4.2)$$

$$B - L : (\kappa, \kappa_n) = (0, -1), \quad g_{Z'}^{(e)} = -g_{Z'}, \quad (4.3)$$

$$L_\mu - L_\tau : (\kappa, \kappa_n) = (0, 0), \quad g_{Z'}^{(e)} = -4.4 \cdot 10^{-3} g_{Z'}, \quad (4.4)$$

$$L_e - L_{\mu(\tau)} : (\kappa, \kappa_n) = (1, 0), \quad g_{Z'}^{(e)} = g_{Z'}. \quad (4.5)$$

In Eq. (4.5), we assume that the loop-induced couplings are negligible (if included, they change κ to 0.992 and 0.987 for $L_e - L_\mu$ and $L_e - L_\tau$, respectively) so that $L_e - L_\mu$ and $L_e - L_\tau$ are treated as the same model in our analysis. In Eq. (4.2), κ and κ_n in principle should slightly deviate from 0 according to Tab. 1, with the deviations proportional to $r_m = m_{Z'}^2/m_Z^2$. However, since r_m is extremely small ($\sim 10^{-22}$ for $m_{Z'} \sim 1$ eV), including the small deviation would not cause visible changes in our final results.

By requiring that the energy loss rate is below the maximally allowed limit, we obtain the constraints on ϵ or $g_{Z'}$ for these models in Fig. 4. As is expected from our previous discussions, when $m_{Z'}$ approaches zero, the stellar cooling bounds vanish for the dark photon model and the $L_\mu - L_\tau$ model because the couplings in these models are photon-like. The bounds for $B - L$ and $L_e - L_{\mu(\tau)}$, by contrast, become flat below certain mass scales. This is caused by $\kappa_n \neq 0$ in the $B - L$ model and $\kappa \neq 0$ in the $L_e - L_{\mu(\tau)}$ model. Our results indicate that stellar cooling constraints on generic Z' in the low-mass limit crucially depend on whether the couplings to the medium particles are in alignment with those of the photon.

In addition to the Sun, one can readily apply the above calculations to other stars with much higher core temperatures and core densities such as red giants (RG) and horizontal branch (HB) stars [26]⁸. For RG, we consider the tip of their evolution before He ignition. At this tip, the orders of magnitude of the core temperature and density are $T \sim 10^8$ K and $\rho \sim 10^6$ g/cm³, while the specific values depend on model-specific simulations. According to several samples of such simulations [87, 88], we vary the core temperature and density in the range $T \in [10^{7.5}, 10^{8.0}]$ K and $\rho \in [10^{5.5}, 10^{6.0}]$ g/cm³. This corresponds to the green bands in Fig. 4. For HB stars in which the ignited He is burning, the core density

⁸See Chapter 2.1.3, Figs. 2.4 and 2.6 therein.

decreases to $\rho \sim 10^4 \text{g/cm}^3$ while the core temperature remains roughly the same after He ignition. According to Ref [26], we vary the core temperature and density in the range $T \in [0.6, 1.2] \times 10^8 \text{K}$ and $\rho \in [10^{3.6}, 10^{4.2}] \text{g/cm}^3$, corresponding to the orange bands in Fig. 4. For both RG and HB stars, we assume that the energy loss rate at the core should be less than $10 \text{erg g}^{-1} \text{sec}^{-1}$ to maintain the agreement between the standard theory and the observations. The chemical composition at the core is assumed to be dominated by He.

In Fig. 4, we also include existing bounds from the fifth-force searches [59] and the observation of supernova 1987A [45, 85] for comparison. The supernova bound for the dark photon model, taken from [45], exhibits a very different low-mass limit compared to those taken from [85]. This is due to the photon-like coupling and the cancellation previously discussed. For $L_\mu - L_\tau$, this cancellation could also be present in supernovae but it should disappear when supernova muons are taken into account [85]. As for bounds from the fifth-force searches, they cannot be applied to photon-like couplings due to the cancellation between positive and negative charge contributions in normal matter.

In the presented mass range, there could also be other laboratory bounds from e.g. neutrino-electron scattering [65, 89] and electron and muon $g - 2$ (see e.g. [5]). These bounds are only relevant when $g_{Z'}$ or ϵ is at least above 10^{-5} so they are not included in the figure. Beam dump bounds (see e.g. [90]) are irrelevant when $m_{Z'} < 2m_e$ because Z' cannot decay to the lightest charged particle.

5 Conclusions

Dark photons and other dark gauge bosons, generically denoted by Z' in this work, could be produced in a hot and dense stellar medium, causing additional energy loss which has been used to derive one of the most constraining bounds on these hypothetical particles.

We show that the production rate of Z' in the low-mass limit crucially depends on how close its couplings are to the photon-like limit, as illustrated in Fig. 3. Consequently, the stellar cooling bounds on Z' from different models can be very different, as shown in Fig. 4.

For $B - L$ and $L_e - L_{\mu(\tau)}$ models with $m_{Z'} \lesssim 10 \text{keV}$, the gauge coupling $g_{Z'}$ is constrained by the solar model to be at least below 4.1×10^{-10} and 3.9×10^{-11} , respectively. The constraints would be much stronger if $m_{Z'}$ is in the resonant production region, or if one considers RG and HB stars, albeit subject to more astrophysical uncertainties. For dark photon and $L_\mu - L_\tau$ models, the effective couplings generated via kinetic mixing or loop diagrams are photon-like. Hence the lower bounds on ϵ or $g_{Z'}$ for these two models are always mass-dependent.

Our model-specific bounds derived from stellar cooling might be of importance to a variety of studies on new light particles at the intensity frontier and in cosmology.

Acknowledgments

We would like to thank Xuheng Luo for inspiring discussions on dark photon mixing in a medium, and Evgeny Akhmedov for helpful clarification on photon scattering issues. This

work is supported in part by the National Natural Science Foundation of China under grant No. 12141501.

A Transformation from the original basis to the physical basis

In this appendix, we present the detail of how the original basis is transformed to the physical basis. As has been briefly described below Eq. (2.1), the transformation involves two steps. First one needs to canonicalize the kinetic terms via a linear non-unitary transformation, denoted by \mathbb{L} , and then diagonalize the mass matrix of gauge bosons by a unitary transformation, denoted by \mathbb{O} . The two steps are formulated as follows:

$$\hat{\mathbf{V}} \xrightarrow{\mathbb{L}} \mathbf{V} \xrightarrow{\mathbb{O}} \mathbf{V}_{\text{ph}}, \quad \mathbf{V} = \mathbb{L}\hat{\mathbf{V}}, \quad \mathbf{V}_{\text{ph}} = \mathbb{O}\mathbf{V}, \quad (\text{A.1})$$

where

$$\hat{\mathbf{V}} \equiv (W_1, W_2, W_3, \hat{B}, \hat{X})^T, \quad (\text{A.2})$$

$$\mathbf{V} \equiv (W_1, W_2, W_3, B, X)^T, \quad (\text{A.3})$$

$$\mathbf{V}_{\text{ph}} \equiv (W_1, W_2, A, Z, Z')^T. \quad (\text{A.4})$$

The specific forms of \mathbb{L} and \mathbb{O} in Eq. (A.1) are given as follows [65]:

$$\mathbb{L} = \begin{pmatrix} \mathbb{I}_3 & & \\ & 1 & \epsilon \\ & 0 & \sqrt{1-\epsilon^2} \end{pmatrix}, \quad \mathbb{O} = \begin{pmatrix} \mathbb{I}_2 & & \\ & s_W & c_W & 0 \\ & c_W c_\theta & -s_W c_\theta & -s_\theta \\ & c_W s_\theta & -s_W s_\theta & c_\theta \end{pmatrix}, \quad (\text{A.5})$$

where \mathbb{I}_n is an $n \times n$ identity matrix, $(s_W \ c_W) \equiv (\sin \theta_W, \cos \theta_W)$ with θ_W the Weinberg angle, and $(s_\theta \ c_\theta) \equiv (\sin \theta, \cos \theta)$. The angle θ , to be determined later, is similar to θ_W in the sense that it describes how much the neutral massive boson of $SU(2)_L$ mixes with $U(1)_X$ instead of $U(1)_Y$. Hence the orthogonal transformation \mathbb{O} can be regarded as a generalized Weinberg rotation in the $SU(2)_L \times U(1)_Y \times U(1)_X$ model, with two angles instead of one.

The \mathbb{T} matrix in Eq. (2.3) is given by

$$\mathbb{T} = \mathbb{O} \cdot \mathbb{L}. \quad (\text{A.6})$$

Note that the specific forms of \mathbb{L} and \mathbb{O} are not unique because $(\mathbb{L}, \mathbb{O}) \rightarrow (\mathbb{L}', \mathbb{O}') = (\mathbb{A} \cdot \mathbb{L}, \mathbb{O} \cdot \mathbb{A}^T)$ with an arbitrary orthogonal matrix \mathbb{A} ($\mathbb{A} \cdot \mathbb{A}^T = 1$) can always canonicalize the kinetic terms and diagonalize the mass matrix. Only their product $\mathbb{T} = \mathbb{O} \cdot \mathbb{L} = \mathbb{O}' \cdot \mathbb{L}'$ is unique.

The angle θ depends on the mass matrix of gauge bosons. If the $U(1)_X$ gauge boson acquires a mass via the Stückelberg mechanism or some dark-sector Higgses which are SM singlets, then there is no mass mixing between \hat{X} and \hat{B} , but the \mathbb{L} transformation causes mass mixing between X and B . After the \mathbb{O} transformation, the mass matrix is re-diagonalized and θ is determined by [65]

$$\tan \theta = \frac{\epsilon m_Z^2 s_W}{m_{Z'}^2 - m_Z^2} + \mathcal{O}(\epsilon^2). \quad (\text{A.7})$$

If the $U(1)_X$ gauge boson acquires its mass via Higgs doublets, then there would be mass mixing in the $\hat{\mathbf{V}}$ basis. After the \mathbb{L} and \mathbb{O} transformations, $\tan\theta$ receives an additional contribution almost independent of ϵ , i.e. the mass mixing depends not only on ϵ but also on additional parameters. In this case, we can treat θ as a free parameter.

The gauge interactions in the $\hat{\mathbf{V}}$ basis read

$$\mathcal{L} \supset \sum_{\psi} \bar{\psi} \gamma^{\mu} \mathbf{Q} \hat{\mathbf{V}}_{\mu} \psi, \quad (\text{A.8})$$

where

$$\mathbf{Q} \equiv \left(g \frac{\sigma_1}{2}, g \frac{\sigma_2}{2}, g \frac{\sigma_3}{2}, g' Q_Y, g_{Z'} Q_X \right). \quad (\text{A.9})$$

After the transformation $\hat{\mathbf{V}} \rightarrow \mathbf{V}_{\text{ph}} = \mathbb{T} \hat{\mathbf{V}}$, one obtains the gauge interactions in the physical (\mathbf{V}_{ph}) basis. It is straightforward to see that the charged-current interactions in the SM are not modified. So we are only concerned with the interactions of A , Z , and Z' . The result is

$$\mathcal{L} \supset e Q_{\text{em}}^{(\psi)} \bar{\psi} A \psi + g_Z^{(\psi)} \bar{\psi} Z \psi + g_{Z'}^{(\psi)} \bar{\psi} Z' \psi, \quad (\text{A.10})$$

which implies that the electromagnetic interactions remain the same as in the SM. The effective couplings $g_Z^{(\psi)}$ and $g_{Z'}^{(\psi)}$ are given by

$$g_Z^{(\psi)} = c_{\theta} g \left[c_W Q_{\text{em}}^{(\psi)} - \frac{Q_Y^{(\psi)}}{c_W} \right] - s_{\theta} \left[g_{Z'} Q_X^{(\psi)} - g Q_Y^{(\psi)} \frac{s_W}{c_W} \epsilon \right] + \mathcal{O}(\epsilon^2), \quad (\text{A.11})$$

$$g_{Z'}^{(\psi)} = s_{\theta} g \left[c_W Q_{\text{em}}^{(\psi)} - \frac{Q_Y^{(\psi)}}{c_W} \right] + c_{\theta} \left[g_{Z'} Q_X^{(\psi)} - g Q_Y^{(\psi)} \frac{s_W}{c_W} \epsilon \right] + \mathcal{O}(\epsilon^2). \quad (\text{A.12})$$

If the kinetic mixing term is the only source of mass mixing, then we can apply Eq. (A.7) to obtain the expressions of $g_Z^{(\psi)}$ and $g_{Z'}^{(\psi)}$ in Tab. 1.

B Medium-induced kinetic mixing rederived from coherent scattering

As we have discussed in Sec. 3.1, coherent scattering of γ/Z' with charged particles in a medium causes medium-induced mixing between γ and Z' . In finite-temperature/density field theories, this can be obtained by computing the following diagram

$$\text{Diagram: } \gamma \text{ (wavy line) } \rightarrow \text{Loop (circle with } f \text{)} \rightarrow Z' \text{ (wavy line)} = \Pi_{\gamma-(f)-Z'}^{\mu\nu}, \quad (\text{B.1})$$

using medium-modified fermion propagators in the loop. And the result is essentially the well-known plasmon masses given in Eq. (3.3) with $Q_f^2 e^2 \rightarrow Q_f e g_{Z'}^{(f)}$.

Here we would like to rederive it from the coherent scattering of γ/Z' with medium particles. By directly computing the following diagrams

$$\text{Diagram 1: } \gamma \text{ (wavy line) } \rightarrow \text{Feynman diagram with } f \text{ (fermion) and } Z' \text{ (wavy line)} + \text{Diagram 2: } \gamma \text{ (wavy line) } \rightarrow \text{Feynman diagram with } f \text{ (fermion) and } Z' \text{ (wavy line)} = \mathcal{M}_{\mu\nu} \epsilon_{\gamma}^{\mu} \epsilon_{Z'}^{\nu}, \quad (\text{B.2})$$

and assuming that the scattering is coherent among multiple medium particles in a local region, one can obtain the same result, but the rederivation provides a more intuitive understanding of the medium effect.

Let us start with Eq. (B.2) where ϵ_γ and $\epsilon_{Z'}$ denote the polarization vectors of γ and Z' respectively. The fermionic part of Eq. (B.2) reads

$$\mathcal{M}^{\mu\nu} = eQ_f g_{Z'}^{(f)} \bar{u} \left[\gamma^\nu \frac{1}{\not{p}_a - m_f} \gamma^\mu + \gamma^\mu \frac{1}{\not{p}_b - m_f} \gamma^\nu \right] u, \quad (\text{B.3})$$

where p_a and p_b denote the momentum of the internal fermion propagator of the first and second diagrams respectively. As a condition of coherence, the momentum transfer from the photon to the medium particle should be sufficiently small. It should be well below the inverse of the radius of the local region maintaining coherency. For simplicity, we take the zero limit of the momentum transfer so that the initial γ and the final Z' have exactly the same momentum. Under this limit, we have $p_a^\mu = p^\mu + k^\mu$ and $p_b^\mu = p^\mu - k^\mu$ where k^μ and p^μ are the momenta of γ and f respectively. Then after applying on-shell conditions ($p^2 = m_f^2$, $\not{p}u = m_f u$, $\bar{u}\not{p} = \bar{u}m_f$), Eq. (B.3) becomes

$$\mathcal{M}^{\mu\nu} = eQ_f g_{Z'}^{(f)} \frac{4k \cdot p (j^\nu k^\mu + j^\mu k^\nu - j \cdot k g^{\mu\nu}) - 2k^2 (j^\nu p^\mu + j^\mu p^\nu)}{4(k \cdot p)^2 - (k^2)^2}, \quad (\text{B.4})$$

with

$$j^\mu \equiv \bar{u} \gamma^\mu u. \quad (\text{B.5})$$

Given the amplitude $\mathcal{M}^{\mu\nu}$, it is straightforward to obtain the corresponding effective Lagrangian in the momentum space:

$$\mathcal{L}_{\text{eff}} = \mathcal{M}^{\mu\nu} |_{j \rightarrow J} A_\mu Z'_\nu, \quad (\text{B.6})$$

where

$$J_\mu \equiv \bar{f} \gamma_\mu f. \quad (\text{B.7})$$

Note that J and j have different dimensions, $J \sim [E]^3$ vs $j \sim [E]^1$. In a background of a large number of f particles, the expectation value $\langle J_\mu \rangle$ is exactly the classical current of f particles. In particular, for a non-relativistic medium, we have

$$\langle J_\mu \rangle \approx (n_f, 0, 0, 0), \quad (\text{B.8})$$

where n_f is the number density of f . Coherent scattering of γ/Z' with the background particles leads to a background expectation value of $\mathcal{M}^{\mu\nu} |_{j \rightarrow J}$, which gives rise to the medium-induced mixing between γ and Z' :

$$\Pi_{\gamma-(f)-Z'}^{\mu\nu} = \langle \mathcal{M}^{\mu\nu} |_{j \rightarrow J} \rangle. \quad (\text{B.9})$$

Next, we use Eqs. (B.4) and (B.8) to compute $\Pi_{\gamma-(f)-Z'}^{\mu\nu}$ in Eq. (B.9). Since $\mathcal{M}^{\mu\nu}$ is multiplied by $\epsilon_\gamma^\mu \epsilon_{Z'}^\nu$ and $k \cdot \epsilon_\gamma = k \cdot \epsilon_{Z'} = 0$, the $j^\nu k^\mu + j^\mu k^\nu$ term in Eq. (B.4) can be ignored. In addition, we only consider a non-relativistic medium, which implies

$$p^\mu \approx (m_f, 0, 0, 0). \quad (\text{B.10})$$

Since the photon is soft compared to the fermion mass ($k \ll m_f$), we can neglect $(k^2)^2$ in the denominator of Eq. (B.4). From Eqs. (B.10) and (B.8), we have $\langle J \rangle \cdot k / (p \cdot k) = n_f / m_f$. Combining all these together, we obtain

$$\Pi_{\gamma-(f)-Z'}^{\mu\nu} = eQ_f g_{Z'}^{(f)} \left[-\frac{n_f}{m_f} g^{\mu\nu} - \frac{k^2}{2(k \cdot p)^2} (\langle J^\nu \rangle p^\mu + \langle J^\mu \rangle p^\nu) \right]. \quad (\text{B.11})$$

Without loss of generality, one can assume that k^μ is in the z -axis direction, $k^\mu = (\omega, 0, 0, |\mathbf{k}|)$ so that the polarization vectors in Eq. (3.2) can be written as follows:

$$\epsilon_{T1}^\mu = (0, 1, 0, 0), \quad \epsilon_{T2}^\mu = (0, 0, 1, 0), \quad \epsilon_L^\mu = \frac{1}{\sqrt{k^2}} (|\mathbf{k}|, 0, 0, \omega). \quad (\text{B.12})$$

Each of them satisfies $k \cdot \epsilon = 0$ and $\epsilon^\mu \epsilon_\mu = -1$.

Applying the decomposition in Eq. (3.2), we obtain

$$\Pi_{\gamma-(f)-Z'}^T = eQ_f g_{Z'}^{(f)} \frac{n_f}{m_f}, \quad (\text{B.13})$$

$$\Pi_{\gamma-(f)-Z'}^L = eQ_f g_{Z'}^{(f)} \frac{n_f}{m_f} \left[1 - \frac{|\mathbf{k}|^2}{\omega^2} \right], \quad (\text{B.14})$$

where we have used $\epsilon_{T1}^\mu p_\mu = 0$, $\epsilon_{T2}^\mu p_\mu = 0$, $\epsilon_L^\mu p_\mu = m_f |\mathbf{k}| / \sqrt{k^2}$, and $\epsilon_L^\mu \langle J_\mu \rangle = n_f |\mathbf{k}| / \sqrt{k^2}$. Therefore, the medium-induced kinetic mixing derived from the coherent scattering theory is identical to that obtained using the finite-temperature/density field theory.

References

- [1] J. Jaeckel and A. Ringwald, *The Low-Energy Frontier of Particle Physics*, *Ann. Rev. Nucl. Part. Sci.* **60** (2010) 405–437, [[1002.0329](#)].
- [2] R. Essig *et al.*, *Working Group Report: New Light Weakly Coupled Particles*, in *Snowmass 2013: Snowmass on the Mississippi*, 10, 2013. [[1311.0029](#)].
- [3] J. Alexander *et al.*, *Dark Sectors 2016 Workshop: Community Report*, 8, 2016. [[1608.08632](#)].
- [4] P. Ilten, Y. Soreq, M. Williams, and W. Xue, *Serendipity in dark photon searches*, *JHEP* **06** (2018) 004, [[1801.04847](#)].
- [5] M. Bauer, P. Foldenauer, and J. Jaeckel, *Hunting All the Hidden Photons*, *JHEP* **07** (2018) 094, [[1803.05466](#)].
- [6] M. Fabbrichesi, E. Gabrielli, and G. Lanfranchi, *The Dark Photon*, [[2005.01515](#)].
- [7] **Belle-II Collaboration**, F. Abudinén *et al.*, *Search for a Dark Photon and an Invisible Dark Higgs Boson in $\mu+\mu^-$ and Missing Energy Final States with the Belle II Experiment*, *Phys. Rev. Lett.* **130** (2023), no. 7 071804, [[2207.00509](#)].
- [8] J. L. Feng, I. Galon, F. Kling, and S. Trojanowski, *ForwArd Search Experiment at the LHC*, *Phys. Rev. D* **97** (2018), no. 3 035001, [[1708.09389](#)].
- [9] **FASER Collaboration**, H. Abreu *et al.*, *First Direct Observation of Collider Neutrinos with FASER at the LHC*, [[2303.14185](#)].
- [10] S. Alekhin *et al.*, *A facility to Search for Hidden Particles at the CERN SPS: the SHiP physics case*, *Rept. Prog. Phys.* **79** (2016), no. 12 124201, [[1504.04855](#)].

- [11] S. Gardner, R. J. Holt, and A. S. Tadepalli, *New Prospects in Fixed Target Searches for Dark Forces with the SeaQuest Experiment at Fermilab*, *Phys. Rev. D* **93** (2016), no. 11 115015, [[1509.00050](#)].
- [12] A. Berlin, S. Gori, P. Schuster, and N. Toro, *Dark Sectors at the Fermilab SeaQuest Experiment*, *Phys. Rev. D* **98** (2018), no. 3 035011, [[1804.00661](#)].
- [13] J. P. Chou, D. Curtin, and H. J. Lubatti, *New Detectors to Explore the Lifetime Frontier*, *Phys. Lett. B* **767** (2017) 29–36, [[1606.06298](#)].
- [14] **MATHUSLA Collaboration**, C. Alpigiani *et al.*, *An Update to the Letter of Intent for MATHUSLA: Search for Long-Lived Particles at the HL-LHC*, [2009.01693](#).
- [15] A. Fradette, M. Pospelov, J. Pradler, and A. Ritz, *Cosmological Constraints on Very Dark Photons*, *Phys. Rev. D* **90** (2014), no. 3 035022, [[1407.0993](#)].
- [16] J. Berger, K. Jedamzik, and D. G. E. Walker, *Cosmological Constraints on Decoupled Dark Photons and Dark Higgs*, *JCAP* **11** (2016) 032, [[1605.07195](#)].
- [17] S. Knapen, T. Lin, and K. M. Zurek, *Light Dark Matter: Models and Constraints*, *Phys. Rev. D* **96** (2017), no. 11 115021, [[1709.07882](#)].
- [18] P. Agrawal, N. Kitajima, M. Reece, T. Sekiguchi, and F. Takahashi, *Relic Abundance of Dark Photon Dark Matter*, *Phys. Lett. B* **801** (2020) 135136, [[1810.07188](#)].
- [19] S. D. McDermott and S. J. Witte, *Cosmological evolution of light dark photon dark matter*, *Phys. Rev. D* **101** (2020), no. 6 063030, [[1911.05086](#)].
- [20] J. Coffey, L. Forestell, D. E. Morrissey, and G. White, *Cosmological Bounds on sub-GeV Dark Vector Bosons from Electromagnetic Energy Injection*, *JHEP* **07** (2020) 179, [[2003.02273](#)].
- [21] E. G. M. Ferreira, *Ultra-light dark matter*, *Astron. Astrophys. Rev.* **29** (2021), no. 1 7, [[2005.03254](#)].
- [22] H. An, F. P. Huang, J. Liu, and W. Xue, *Radio-frequency Dark Photon Dark Matter across the Sun*, *Phys. Rev. Lett.* **126** (2021), no. 18 181102, [[2010.15836](#)].
- [23] H. An, X. Chen, S. Ge, J. Liu, and Y. Luo, *Searching for Ultralight Dark Matter Conversion in Solar Corona using LOFAR Data*, [2301.03622](#).
- [24] G. G. Raffelt and D. S. P. Dearborn, *Bounds on Hadronic Axions From Stellar Evolution*, *Phys. Rev. D* **36** (1987) 2211.
- [25] G. G. Raffelt, *Astrophysical methods to constrain axions and other novel particle phenomena*, *Phys. Rept.* **198** (1990) 1–113.
- [26] G. G. Raffelt, *Stars as laboratories for fundamental physics: The astrophysics of neutrinos, axions, and other weakly interacting particles*. University of Chicago Press, 1996.
- [27] G. G. Raffelt, *Particle physics from stars*, *Ann. Rev. Nucl. Part. Sci.* **49** (1999) 163–216, [[hep-ph/9903472](#)].
- [28] S. Davidson, S. Hannestad, and G. Raffelt, *Updated bounds on millicharged particles*, *JHEP* **05** (2000) 003, [[hep-ph/0001179](#)].
- [29] J. Redondo, *Helioscope Bounds on Hidden Sector Photons*, *JCAP* **07** (2008) 008, [[0801.1527](#)].
- [30] H. An, M. Pospelov, and J. Pradler, *New stellar constraints on dark photons*, *Phys. Lett. B* **725** (2013) 190–195, [[1302.3884](#)].

- [31] J. Redondo and G. Raffelt, *Solar constraints on hidden photons re-visited*, *JCAP* **08** (2013) 034, [[1305.2920](#)].
- [32] N. Vinyoles, A. Serenelli, F. L. Villante, S. Basu, J. Redondo, and J. Isern, *New axion and hidden photon constraints from a solar data global fit*, *JCAP* **10** (2015) 015, [[1501.01639](#)].
- [33] E. Hardy and R. Lasenby, *Stellar cooling bounds on new light particles: plasma mixing effects*, *JHEP* **02** (2017) 033, [[1611.05852](#)].
- [34] X. Chu, J.-L. Kuo, J. Pradler, and L. Semmelrock, *Stellar probes of dark sector-photon interactions*, *Phys. Rev. D* **100** (2019), no. 8 083002, [[1908.00553](#)].
- [35] W. DeRocco, P. W. Graham, and S. Rajendran, *Exploring the robustness of stellar cooling constraints on light particles*, *Phys. Rev. D* **102** (2020), no. 7 075015, [[2006.15112](#)].
- [36] H. An, M. Pospelov, J. Pradler, and A. Ritz, *New limits on dark photons from solar emission and keV scale dark matter*, *Phys. Rev. D* **102** (2020) 115022, [[2006.13929](#)].
- [37] P. Carena, O. Straniero, B. Döbrich, M. Giannotti, G. Lucente, and A. Mirizzi, *Constraints on the coupling with photons of heavy axion-like-particles from Globular Clusters*, *Phys. Lett. B* **809** (2020) 135709, [[2004.08399](#)].
- [38] F. Capozzi and G. Raffelt, *Axion and neutrino bounds improved with new calibrations of the tip of the red-giant branch using geometric distance determinations*, *Phys. Rev. D* **102** (2020), no. 8 083007, [[2007.03694](#)].
- [39] S. Balaji, P. S. B. Dev, J. Silk, and Y. Zhang, *Improved stellar limits on a light CP-even scalar*, *JCAP* **12** (2022) 024, [[2205.01669](#)].
- [40] Y. Yamamoto and K. Yoshioka, *Stellar cooling limits on light scalar boson revisited*, [2303.03123](#).
- [41] S. Bottaro, A. Caputo, G. Raffelt, and E. Vitagliano, *Stellar limits on scalars from electron-nucleus bremsstrahlung*, [2303.00778](#).
- [42] J. B. Dent, F. Ferrer, and L. M. Krauss, *Constraints on Light Hidden Sector Gauge Bosons from Supernova Cooling*, [1201.2683](#).
- [43] D. Kazanas, R. N. Mohapatra, S. Nussinov, V. L. Teplitz, and Y. Zhang, *Supernova Bounds on the Dark Photon Using its Electromagnetic Decay*, *Nucl. Phys. B* **890** (2014) 17–29, [[1410.0221](#)].
- [44] E. Rrapaj and S. Reddy, *Nucleon-nucleon bremsstrahlung of dark gauge bosons and revised supernova constraints*, *Phys. Rev. C* **94** (2016), no. 4 045805, [[1511.09136](#)].
- [45] J. H. Chang, R. Essig, and S. D. McDermott, *Revisiting Supernova 1987A Constraints on Dark Photons*, *JHEP* **01** (2017) 107, [[1611.03864](#)].
- [46] L. Heurtier and Y. Zhang, *Supernova Constraints on Massive (Pseudo)Scalar Coupling to Neutrinos*, *JCAP* **02** (2017) 042, [[1609.05882](#)].
- [47] P. S. B. Dev, R. N. Mohapatra, and Y. Zhang, *Revisiting supernova constraints on a light CP-even scalar*, *JCAP* **08** (2020) 003, [[2005.00490](#)]. [Erratum: *JCAP* **11**, E01 (2020)].
- [48] D. K. Hong, C. S. Shin, and S. Yun, *Cooling of young neutron stars and dark gauge bosons*, *Phys. Rev. D* **103** (2021), no. 12 123031, [[2012.05427](#)].
- [49] C. S. Shin and S. Yun, *Dark gauge boson production from neutron stars via nucleon-nucleon bremsstrahlung*, *JHEP* **02** (2022) 133, [[2110.03362](#)].

- [50] C. S. Shin and S. Yun, *Dark gauge boson emission from supernova pions*, [2211.15677](#).
- [51] A. Davidson, *$B - L$ as the fourth color within an $SU(2)_L \times U(1)_R \times U(1)$ model*, *Phys. Rev. D* **20** (1979) 776.
- [52] R. N. Mohapatra and R. E. Marshak, *Local $B-L$ Symmetry of Electroweak Interactions, Majorana Neutrinos and Neutron Oscillations*, *Phys. Rev. Lett.* **44** (1980) 1316–1319. [Erratum: *Phys.Rev.Lett.* **44**, 1643 (1980)].
- [53] C. Wetterich, *Neutrino Masses and the Scale of $B-L$ Violation*, *Nucl. Phys. B* **187** (1981) 343–375.
- [54] R. Foot, *New Physics From Electric Charge Quantization?*, *Mod. Phys. Lett. A* **6** (1991) 527–530.
- [55] X. G. He, G. C. Joshi, H. Lew, and R. R. Volkas, *NEW Z -prime PHENOMENOLOGY*, *Phys. Rev. D* **43** (1991) 22–24.
- [56] X.-G. He, G. C. Joshi, H. Lew, and R. R. Volkas, *Simplest Z -prime model*, *Phys. Rev. D* **44** (1991) 2118–2132.
- [57] J. Heeck and W. Rodejohann, *Gauged $L_\mu - L_\tau$ Symmetry at the Electroweak Scale*, *Phys. Rev. D* **84** (2011) 075007, [[1107.5238](#)].
- [58] R. Harnik, J. Kopp, and P. A. N. Machado, *Exploring ν Signals in Dark Matter Detectors*, *JCAP* **07** (2012) 026, [[1202.6073](#)].
- [59] J. Heeck, *Unbroken $B - L$ symmetry*, *Phys. Lett. B* **739** (2014) 256–262, [[1408.6845](#)].
- [60] A. Crivellin, G. D’Ambrosio, and J. Heeck, *Explaining $h \rightarrow \mu^\pm \tau^\mp$, $B \rightarrow K^* \mu^+ \mu^-$ and $B \rightarrow K \mu^+ \mu^- / B \rightarrow K e^+ e^-$ in a two-Higgs-doublet model with gauged $L_\mu - L_\tau$* , *Phys. Rev. Lett.* **114** (2015) 151801, [[1501.00993](#)].
- [61] W. Altmannshofer, S. Gori, S. Profumo, and F. S. Queiroz, *Explaining dark matter and B decay anomalies with an $L_\mu - L_\tau$ model*, *JHEP* **12** (2016) 106, [[1609.04026](#)].
- [62] M. B. Wise and Y. Zhang, *Lepton Flavorful Fifth Force and Depth-dependent Neutrino Matter Interactions*, *JHEP* **06** (2018) 053, [[1803.00591](#)].
- [63] A. Kamada, K. Kaneta, K. Yanagi, and H.-B. Yu, *Self-interacting dark matter and muon $g - 2$ in a gauged $U(1)_{L_\mu - L_\tau}$ model*, *JHEP* **06** (2018) 117, [[1805.00651](#)].
- [64] K. Asai, K. Hamaguchi, N. Nagata, S.-Y. Tseng, and K. Tsumura, *Minimal Gauged $U(1)_{L_\alpha - L_\beta}$ Models Driven into a Corner*, *Phys. Rev. D* **99** (2019), no. 5 055029, [[1811.07571](#)].
- [65] M. Lindner, F. S. Queiroz, W. Rodejohann, and X.-J. Xu, *Neutrino-electron scattering: general constraints on Z' and dark photon models*, *JHEP* **05** (2018) 098, [[1803.00060](#)].
- [66] J. Heeck, M. Lindner, W. Rodejohann, and S. Vogl, *Non-Standard Neutrino Interactions and Neutral Gauge Bosons*, *SciPost Phys.* **6** (2019), no. 3 038, [[1812.04067](#)].
- [67] M. Escudero, D. Hooper, G. Krnjaic, and M. Pierre, *Cosmology with A Very Light $L_\mu - L_\tau$ Gauge Boson*, *JHEP* **03** (2019) 071, [[1901.02010](#)].
- [68] K. Asai, *Predictions for the neutrino parameters in the minimal model extended by linear combination of $U(1)_{L_e - L_\mu}$, $U(1)_{L_\mu - L_\tau}$ and $U(1)_{B-L}$ gauge symmetries*, *Eur. Phys. J. C* **80** (2020), no. 2 76, [[1907.04042](#)].

- [69] A. Esmaili and Y. Farzan, *Explaining the ANITA events by a $L_e - L_\tau$ gauge model*, *JCAP* **12** (2019) 017, [[1909.07995](#)].
- [70] C.-H. Chen and T. Nomura, *Electron and muon $g - 2$, radiative neutrino mass, and $\ell' \rightarrow \ell\gamma$ in a $U(1)_{e-\mu}$ model*, *Nucl. Phys. B* **964** (2021) 115314, [[2003.07638](#)].
- [71] G.-y. Huang, F. S. Queiroz, and W. Rodejohann, *Gauged $L_\mu - L_\tau$ at a muon collider*, *Phys. Rev. D* **103** (2021), no. 9 095005, [[2101.04956](#)].
- [72] B. Holdom, *Two $U(1)$'s and Epsilon Charge Shifts*, *Phys. Lett. B* **166** (1986) 196–198.
- [73] P. Langacker, *The Physics of Heavy Z' Gauge Bosons*, *Rev. Mod. Phys.* **81** (2009) 1199–1228, [[0801.1345](#)].
- [74] E. C. G. Stueckelberg, *Interaction energy in electrodynamics and in the field theory of nuclear forces*, *Helv. Phys. Acta* **11** (1938) 225–244.
- [75] D. Feldman, Z. Liu, and P. Nath, *The Stueckelberg Z -prime Extension with Kinetic Mixing and Milli-Charged Dark Matter From the Hidden Sector*, *Phys. Rev. D* **75** (2007) 115001, [[hep-ph/0702123](#)].
- [76] G. Raffelt and L. Stodolsky, *Mixing of the Photon with Low Mass Particles*, *Phys. Rev. D* **37** (1988) 1237.
- [77] E. Braaten and D. Segel, *Neutrino energy loss from the plasma process at all temperatures and densities*, *Phys. Rev. D* **48** (1993) 1478–1491, [[hep-ph/9302213](#)].
- [78] P. J. Brussaard and H. C. van de Hulst, *Approximation Formulas for Nonrelativistic Bremsstrahlung and Average Gaunt Factors for a Maxwellian Electron Gas*, *Rev. Mod. Phys.* **34** (1962) 507–520.
- [79] X.-J. Xu, Z. Wang, and S. Chen, *Solar neutrino physics*, [2209.14832](#).
- [80] H. A. Weldon, *Simple Rules for Discontinuities in Finite Temperature Field Theory*, *Phys. Rev. D* **28** (1983) 2007.
- [81] N. Vinyoles, A. M. Serenelli, F. L. Villante, S. Basu, J. Bergström, M. C. Gonzalez-Garcia, M. Maltoni, C. Peña Garay, and N. Song, *A new Generation of Standard Solar Models*, *Astrophys. J.* **835** (2017), no. 2 202, [[1611.09867](#)].
- [82] M. Asplund, N. Grevesse, A. J. Sauval, and P. Scott, *The chemical composition of the Sun*, *Ann. Rev. Astron. Astrophys.* **47** (2009) 481–522, [[0909.0948](#)].
- [83] G. D. O. Gann, K. Zuber, D. Bemmerer, and A. Serenelli, *The Future of Solar Neutrinos*, *Ann. Rev. Nucl. Part. Sci.* **71** (2021) 491–528, [[2107.08613](#)].
- [84] P. Gondolo and G. G. Raffelt, *Solar neutrino limit on axions and keV-mass bosons*, *Phys. Rev. D* **79** (2009) 107301, [[0807.2926](#)].
- [85] D. Croon, G. Elor, R. K. Leane, and S. D. McDermott, *Supernova Muons: New Constraints on Z' Bosons, Axions and ALPs*, *JHEP* **01** (2021) 107, [[2006.13942](#)].
- [86] T. Araki, S. Hoshino, T. Ota, J. Sato, and T. Shimomura, *Detecting the $L_\mu - L_\tau$ gauge boson at Belle II*, *Phys. Rev. D* **95** (2017), no. 5 055006, [[1702.01497](#)].
- [87] J.-C. Passy, M.-M. Mac Low, and O. De Marco, *On the survival of brown dwarfs and planets engulfed by their giant host star*, *Astrophys. J. Lett.* **759** (2012) L30, [[1210.0879](#)].
- [88] C. Dessert and Z. Johnson, *Red-giant branch stellar cores as macroscopic dark matter detectors*, *Phys. Rev. D* **106** (2022), no. 10 103034, [[2112.06949](#)].

- [89] S. Bilmis, I. Turan, T. Aliev, M. Deniz, L. Singh, and H. Wong, *Constraints on Dark Photon from Neutrino-Electron Scattering Experiments*, *Phys. Rev. D* **92** (2015), no. 3 033009, [[1502.07763](#)].
- [90] R. Coy and X.-J. Xu, *Probing the muon $g - 2$ with future beam dump experiments*, *JHEP* **10** (2021) 189, [[2108.05147](#)].